

$^{52}\text{Cr}(p, \alpha)^{49}\text{V}$ reaction

P. A. Smith,* J. A. Nolen, Jr., R. G. Markham, and M. A. M. Shahabuddin†

Cyclotron Laboratory and Physics Department, Michigan State University, East Lansing, Michigan 48824

(Received 18 November 1977; revised manuscript received 13 July 1978)

The $^{52}\text{Cr}(p, \alpha)^{49}\text{V}$ reaction has been studied at a bombarding energy of 35 MeV. The qualitative features of the spectra are discussed. These include the population of proton hole states, analog states, and high spin states. The spectra are compared with other pick-up reaction data and the comparison is shown to be a useful tool for identifying positive parity states in this region. Some states which are observed in $^{51}\text{V}(p, t)^{49}\text{V}$ data are not observed in the (p, α) spectra. Distorted-wave calculations using mass three cluster form factors are described and shown to reproduce the experimental angular distributions of the previously known levels. Similar calculations using microscopic form factors also reproduce the shapes of the angular distributions reasonably well. Relative spectroscopic factors for the proton hole states deduced from the microscopic calculations are shown to be in good agreement with zero order shell model predictions. The general trends of the experimental cross sections for the negative parity microscopic states are shown to be reproduced by microscopic calculations assuming $0f_{7/2}^3$ pickup.

NUCLEAR REACTIONS $^{52}\text{Cr}(p, \alpha)$, $E_p=35$ MeV; measured $\sigma(E_x, \theta)$, deduced energy levels; studied reaction mechanism.

I. INTRODUCTION

The (p, α) and (α, p) reactions may prove to be very useful spectroscopic tools. The qualitative features of these reactions are not well documented, with the exception of j -dependence for $\ell=1$ transfers.^{1,2,3,4} With the (p, α) reaction, for example, it is possible to study proton hole states in nuclei that are not accessible by other pick-up reactions, either because the targets for these reactions are unstable or difficult to make. Final nuclei in this class are ^{47}V , ^{51}Mn , ^{55}Co , ^{109}In , and ^{119}Sb . (Refs. 5-10) To understand the spectra of these nuclei, it is necessary to document the properties of the (p, α) reaction on nuclei that have been previously studied with simpler reactions. In this paper the qualitative features of the (p, α) reaction as seen in the $^{52}\text{Cr}(p, \alpha)^{49}\text{V}$ reaction are investigated. The $^{52}\text{Cr}(p, \alpha)^{49}\text{V}$ reaction is a good choice for such a study in the $0f_{7/2}$ shell because ^{49}V has been studied by a number of others.^{5,11-24}

Previous work in this mass region at beam energies above 17 MeV has shown that the simple proton hole states that are populated in single proton pick-up reactions dominate the (p, α) spectra (see references 2 and 25 for example). These states seem to be described reasonably well with seniority-one wave functions. Therefore, we should expect the ^{49}V spectrum to display strong peaks for the $7/2^-$ ground state and the $3/2^+$ and $1/2^+$ sd-shell proton hole states.

In addition to the $T=3/2$ proton hole states, the $T=5/2$ analogs of the hole states in ^{49}Ti should also be populated. These states are not isospin allowed in the $^{50}\text{Cr}(d, ^3\text{He})^{49}\text{V}$ or the $^{50}\text{Cr}(t, \alpha)^{49}\text{V}$ reactions. Experimental observation of analog states with the (p, α) reaction has not been previously demonstrated except for some tentative assignments by Bardin and Rickey²⁶ with Ti targets, and the recent work of Smits and Siemssen.⁹

Multi-particle transfer direct reactions also have additional degrees of freedom which permit the population of high spin states.²⁷ For some time now the $(\alpha, xn\gamma)$ compound nuclear reactions have been used to populate such states, and recently heavy ion induced reactions such as $(^{19}\text{F}, p2n\gamma)$ have been used to find high spin states such as the 12^+ in ^{44}Ti .²⁸ In the (p, α) reaction, if two $0f_{7/2}$

neutrons and a $0f_{7/2}$ proton are picked up, it is possible to reach final states via j^π transfers of up to $19/2^-$. The (p, α) reaction on ^{51}V could, in principle, directly populate a 12^+ state in ^{48}Ti . If the proton comes from the $0d_{3/2}$ orbit, $15/2^+$ is the maximum j^π transfer. A study of the $^{90,92,94,96}\text{Zr}(p, \alpha)^{87,89,91,95}\text{Y}$ reactions has concentrated on this aspect of the reaction.²⁹ Spins up to $15/2^-$ were observed in that work. The maximum coupling of $0d_{5/2}^-$, which is $13/2^+$, has been observed in $^{12}\text{C}(\alpha, p)^{15}\text{N}$, and $^{16}\text{O}(\alpha, p)^{\text{F}}$ (see Refs. 30 and 31).

The best known feature of the (p, α) and (α, p) reactions is the strong j -dependence exhibited by $\ell=1$ transfers. The $1/2^-$ angular distribution is characterized by deep minima, while the $3/2^-$ angular distribution is featureless. This is an appealing feature for making j^π assignments for unknown states. Lee et al.¹ have shown that the j -dependence is a result of spin-orbit coupling in the proton optical potential. The j -dependence for the $j^\pi=1/2^-, 3/2^-$ spin-orbit pair is qualitatively reproduced by Distorted Wave Born approximation (DWBA) calculations independent of the details of the form factor used (see references 1, 3, 29 for examples). However, the reliability of j -dependence for high ℓ -values is not so clear. Studies of the $\ell=2$ and 3 transfers are confusing.^{4,32} Much of this confusion is apparently the result of important structure effects in the sd-shell. A study of the $^{24,26}\text{Mg}(p, \alpha)^{21,23}\text{Na}$ reactions shows that the angular distributions for states with the same j^π values sometimes have very different shapes.³³ It would seem that j -dependence will only be a useful tool in those mass regions where the shapes of the angular distributions are insensitive to the detailed structures of the states. This may be the case for targets that are heavier than those in the sd-shell.

The most common method of using the DWBA to predict the shapes of angular distributions of (p, α) and (α, p) studies has been with zero-range calculations employing mass three cluster form factors. For $A \geq 40$ these calculations fit the data reasonably well in most cases. In regions where nuclear structure does not affect the shapes of the angular distributions, it may be possible to use these calculations to make j^π assignments.^{29,34}

Microscopic reaction models for 3-nucleon transfer reactions have been developed, but they have not been

applied extensively to data. Such models may make it possible to predict both shapes and magnitudes of the angular distributions even when nuclear structure effects are important, provided detailed wave functions are utilized. A recently developed semi-microscopic model^{9,35} is very useful in understanding the influence of coherence effects on (p,α) cross sections in mass regions where detailed structure does not affect angular distributions.

In the sections to follow we will document the general features of the $^{52}\text{Cr}(p,\alpha)$ reaction, try to evaluate the reliability of the $\ell=2$ and $\ell=3$ j -dependence for this case, check the use of the DWBA using cluster form factors, and test DWBA calculations based on microscopic form factors³⁶ generated with an adaptation of the Bayman and Kallio technique.³⁷

II. EXPERIMENTAL METHOD AND DATA

The 35 MeV proton beam from the Michigan State University isochronous cyclotron was used to bombard an isotopically enriched ^{52}Cr target. The reaction products were momentum analyzed in an Enge split-pole spectrograph and detected with the delay line counter developed by Markham and Robertson.³⁸ Position and energy loss information were taken from this counter, while a plastic scintillator placed behind the counter was used to obtain particle time-of-flight information relative to the cyclotron r.f. structure. The α -particles were unambiguously identified by their energy loss in the counter and their time-of-flight. An overall energy resolution of 20 keV FWHM was obtained with this system using a solid angle of 2.0 msr and a beam current of approximately 2.5 μA .

The target thicknesses, typically 20 to 40 $\mu\text{g}/\text{cm}^2$, were measured by comparing proton elastic scattering near the second maximum of the elastic scattering angular distribution to the results of optical model predictions. The targets were made by reducing $^{52}\text{Cr}_2\text{O}_3$ with tantalum and simultaneously evaporating the liberated Cr onto 20 $\mu\text{g}/\text{cm}^2$ carbon backings. A target thickness of $\leq 50 \mu\text{g}/\text{cm}^2$ was obtainable by this technique.

A few spectra were also recorded on photographic emulsions in order to obtain better resolution and more

accurate values for the excitation energies. One of these spectra with a resolution of about 10 keV FWHM is shown in Figure 1. The three strong peaks are the $7/2^-$ ground state, the $3/2^+$ proton-hole state at 0.748 MeV, and 1.646 MeV, $1/2^+$ proton-hole state. In addition, there is a tall peak due to the 1.95 MeV $5/2^+$ hole state in ^{29}P which is the result of ^{32}S impurity in the target. The wide peak near channel 1650 is the ^{13}N ground state, which is kinematically out of focus.

To observe the $T=5/2$ proton-hole analog states, separate spectra of the higher excitation region were recorded as shown in Figure 2. These data were recorded with the 25 cm Markham-Robertson detector³⁸ before the newer 50 cm version was completed. At forward angles the break-up of ^9B , made by the $^{12}\text{C}(p,\alpha)^9\text{B}$ reaction, causes a large background as can be seen in the top half of Figure 2. The bottom half of the Figure contains the 55° spectrum where the alphas from ^9B have kinematically shifted out of the way. The three peaks labeled $7/2^-$, $1/2^+$, and $3/2^+$ are the $T=5/2$ analogs of states in ^{49}Ti .

Candidates for high spin states can be identified by looking for large peaks in back angle spectra. Peaks due to levels which have lower spins become weak as the angle increases, while the higher spin states have relatively flat angular distributions. The peak at 4.797 MeV is a good candidate for a high spin state. In the spectrum at 12° it is comparable to many other states, while at 60° it is the strongest peak.

The angular distributions of levels observed in this experiment are displayed in Figures 3, 4, and 5. The typical cross sections are on the order of 100 $\mu\text{b}/\text{sr}$ for strong states at forward angles down to less than 10 $\mu\text{b}/\text{sr}$ for the weaker states. The calculated curves also included in Figures 3 and 5 are discussed later.

III. DISCUSSION OF DATA AND ANALYSIS

A. Comparison with Other Experiments

A summary of the energy levels observed in this experiment is presented in Table I, together with a summary of data from the literature. Most of the j^π values are a consensus of the literature with our results being gen-

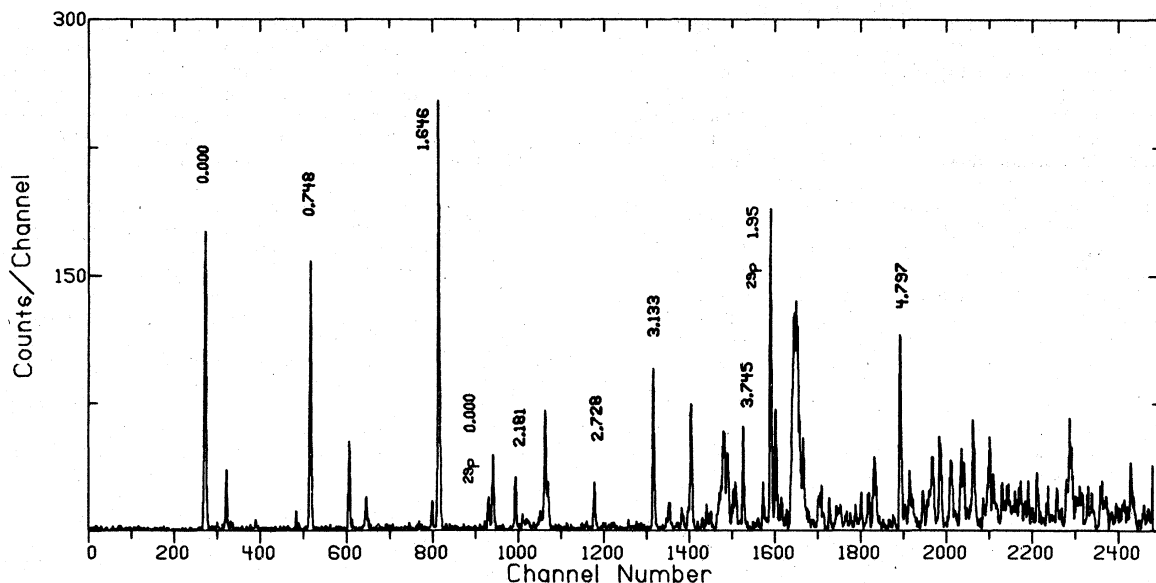


FIG. 1. A $^{52}\text{Cr}(p,\alpha)^{49}\text{V}$ spectrum recorded at 16° on a nuclear track plate with a resolution of 10 keV at a beam energy of 35 MeV.

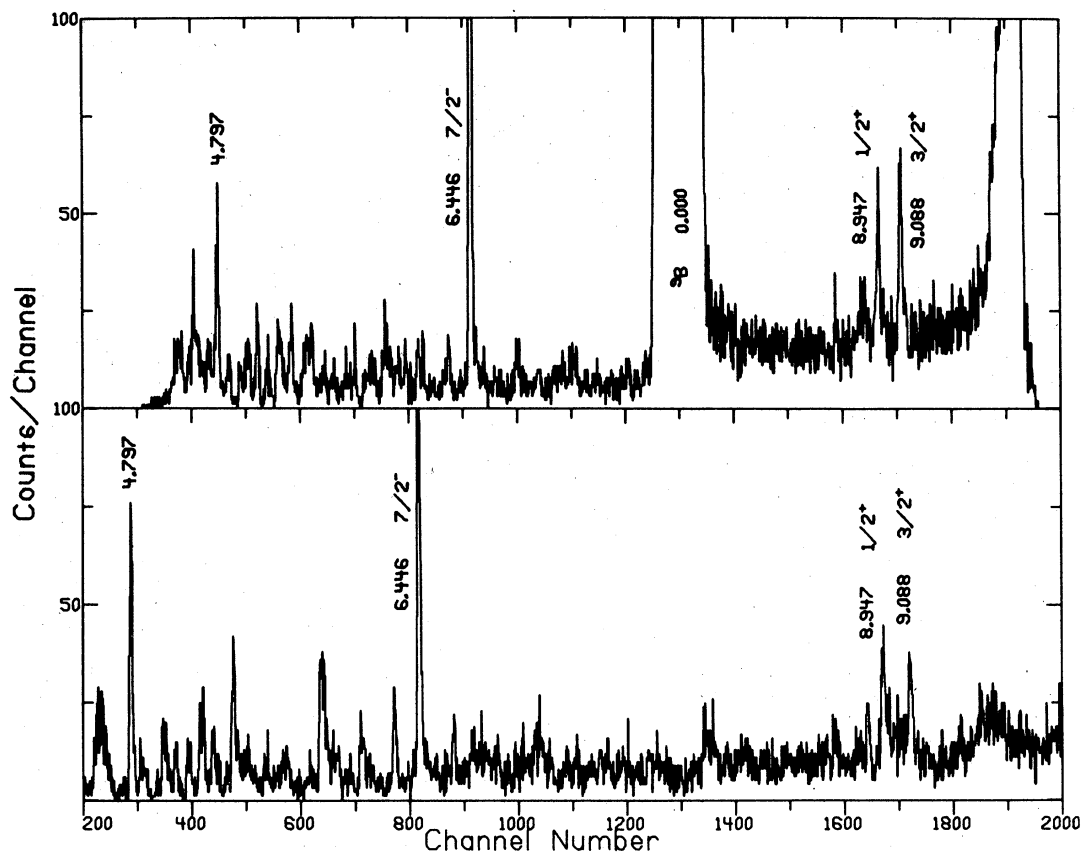


FIG. 2. Two $^{52}\text{Cr}(p,\alpha)^{49}\text{V}$ spectra recorded with the delay-line counter showing the yields to states at higher excitation energies. The strong state at 4.797 MeV and three isobaric analog states are indicated. The upper spectrum was recorded at 24° and the lower at 55° .

erally consistent with those assignments. The assignments explicitly made from this work are the tentative "high spin" assignments and the j^π , T assignments for the three analog states.

To begin the discussion of Table 1, consider the columns labeled (p, α) and (p,t). Beginning at the top of the (p,t) column and working down, it is seen that the 0.748 MeV state is the first one not seen in the (p,t) reaction. This is the $3/2^+$ state due to a proton hole in the $0d_{3/2}$ orbit. The next level not observed in the (p,t) reaction is the 1.141 MeV, $5/2^+$ state. Furthermore the 1.602 MeV, $7/2^+$ and 1.646 MeV, $1/2^+$ levels are not observed in the (p,t) data. All these levels are seen in the (p, α) experiment. A summary of the levels seen in the (p, α) data that are not in the (p,t) data is given in Table 2. Table 2 contains every known positive parity state in ^{49}V except the 2.179 MeV, $9/2^+$ state which cannot be resolved from the 2.183 MeV, $7/2^+$ state. Furthermore, there are no known negative parity levels in this list. This comparison indicates that parity assignments can be made with reasonable certainty by such a comparison.

Reversing the comparison, there are levels seen in the (p,t) experiment that are not seen in the (p, α) spectra. The first of these is the 1.661 MeV, $3/2^+$ state. In addition, all the $5/2^-$ levels are so weak in the (p, α) reaction as to be virtually absent. If the (t, α) results are included in the comparison, it is found that there are

levels excited by the (t, α) reaction that are not in the (p, α) column. Some of these levels are in both the (p,t) and (t, α) data, but not in the (p, α) column. Behaviour of this nature can only be explained by a microscopic model which contains the coherent sum over all the di-neutron couplings and all the three nucleon configurations. Table 3 is a summary of levels missing from the (p, α) spectra.

Extensive (α ,p γ)¹⁶ research has shown that the peak at 3.133 MeV in the (p, α) spectra is a doublet with less than 1 keV separation. Nonetheless, the angular distribution for this peak is nearly the same as that for the 1.021 MeV state, possibly indicating that one of these states has $j=11/2^-$. The same authors have given a $15/2^-$ assignment to the levels at 2.263 MeV and 2.728 MeV. Unfortunately $17/2^-$ and $19/2^-$ levels have not been found by gamma-ray spectroscopy. In the case of positive parity the highest definite j^π assignment is $9/2^+$. The two $15/2^-$ levels are observed very weakly, as indicated in Figure 4.

The angular distribution of the 4.797 MeV level is similar to the angular distribution of the $15/2^-$ state at 2.728 MeV, indicating that a $15/2^-$ assignment should be favored for the former level. Further evidence for this assignment is the likeness of this angular distribution to that for the very strong $15/2^-$ state observed recently in the $^{40}\text{Ca}(\alpha,p)^{43}\text{Sc}$ reaction.³⁹ The angular distribution for the 3.745 MeV state appears to be unique so that a

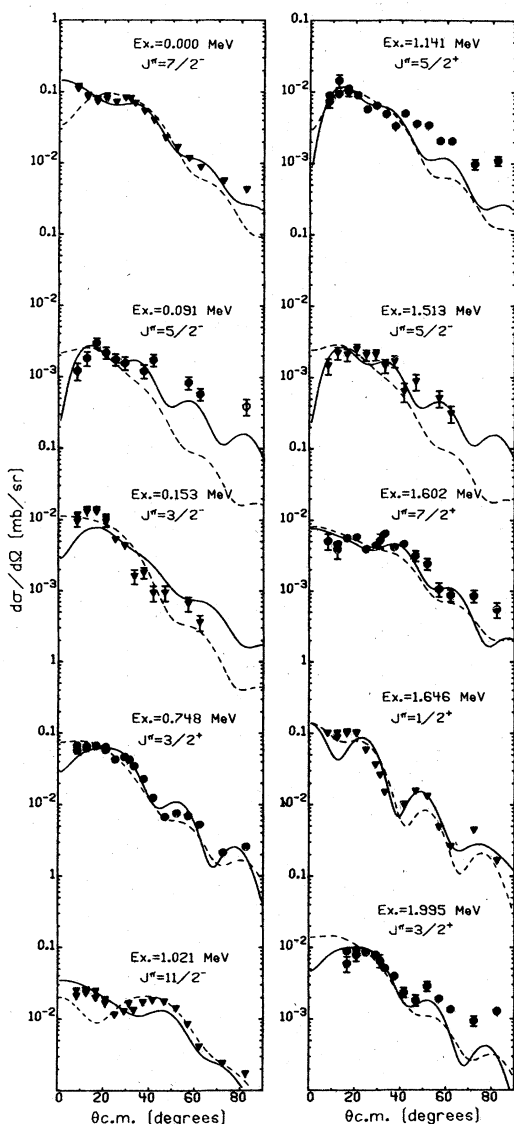


FIG. 3. Angular distributions for the $^{52}\text{Cr}(p,\alpha)^{49}\text{V}$ reaction to below 2 MeV. The solid curves are DWBA calculations with cluster model form factors and the dashed curves are similar calculations with microscopic form factors.

spin assignment cannot be made by comparison to a known shape. The angular distribution for the 3.612 MeV level is not shown in Figure 4 because it was not resolved in the counter spectra.

Although the high spin levels which are observed here have not been previously reported in α -induced gamma-ray coincidence experiments, we can be reasonably sure that the 3.612 MeV level has negative parity and the 3.745 MeV state has positive parity. Neither of these assignments is unambiguous since the 3.612 MeV peak is too broad at forward angles to be a single state and the 3.745 MeV level has been reported in the (p,γ) data,

indicating a possible low spin assignment at this energy. Furthermore, a recent heavy ion induced γ -ray experiment suggests a $19/2^-$ assignment to a level at 3.741 MeV.⁴⁰ Neither the 3.612 MeV state nor the 4.797 MeV state is particularly close to the McCullen, Bayman, and Zamick (MBZ)⁴¹ predictions for high spin negative parity states. The predicted energies for $15/2^-$ levels are 2.575 MeV, 3.544 MeV, 4.083 MeV, and 4.964 MeV. Since the predicted excitation for the first $15/2^-$ is nearly 300 keV too high, while the second one is over-predicted by about 800 keV, it is not surprising that our high spin candidate is not near the MBZ predictions. The MBZ predictions for the two $19/2^-$ levels with the largest "triton" components are 4.331 MeV and 5.143 MeV. More calculations which are similar to the MBZ calculations have been performed recently with improved interactions.⁴² The results of these calculations show that the lowest $15/2^-$ energy is reproduced within 50 keV if the interactions are taken from ^{54}Co data. Unfortunately, the comparison of experiment to the theory remains unclear because of the high density of states above 3 MeV excitation.

B. j-dependence

The striking j-dependence for $\ell=1$ transitions was not observed in this experiment because the only known $1/2^-$ level is obscured by the $1/2^+$ proton hole state. The $3/2^-$ level at 0.153 MeV excitation does exhibit the usual featureless fall-off.

Two $3/2^+$ and two $5/2^+$ states have been observed, but the $5/2^+$ state at 2.386 MeV cannot be resolved sufficiently well to obtain its angular distribution. The other three $\ell=2$ angular distributions are shown in Figure 3, where it is seen that there is no strong j-dependence in this case, though the angular distributions are somewhat different. There are not enough data to determine if the difference is due to j-dependence or is the result of structure effects. Additional data in this mass region are necessary to document the degree of and stability of the $\ell=2$ j-dependence.

The spin-orbit pair with $\ell=3$ is observed. Three $5/2^-$ levels are populated weakly, and even though the cross section is less than $1 \mu\text{b/sr}$ at many points, the 0.091 MeV and 1.513 MeV levels were strong enough to obtain angular distributions. The lowest $5/2^-$ level in many nuclei in this mass region is known to be primarily a seniority three proton state,^{41,42,43} which, if pure, should not be populated in this experiment. Its weak population may indicate a more complicated wave function. The $7/2^-$ states are observed at 0.000 MeV, 3.240 MeV, and 6.446 MeV excitation. The angular distribution for the 3.240 MeV level is somewhat different from the other $7/2^-$ levels. The $7/2^-$ assignment for this state is unambiguous since it is based on the $\ell=0$ angular distribution observed in the $^{51}\text{V}(p,t)^{49}\text{V}$ reaction.¹¹ It seems that this is a case where structure effects can be as strong as j-dependence, or that this angular distribution is an anomaly caused by an unresolved doublet. If the abnormal angular distribution is neglected the j-dependence appears to be manifested in the forward angles. The $5/2^-$ tends to go down as the angle decreases, while the $7/2^-$ rises. Two other $7/2^-$ states are also populated, but, unfortunately, they are members of close doublets.

Only one $\ell=4$ transfer is resolved, leading to the $7/2^+$ state at 1.602 MeV. The $9/2^+$ level at 2.179 MeV may be populated, but cannot be resolved from the $7/2^+$ state at 2.183 MeV.

There are known $9/2^-$ and $11/2^-$ levels in the first two MeV of excitation. The $11/2^-$ is observed, but there is no evidence for the $9/2^-$. Another $9/2^-$ state located at 2.354 MeV is barely visible in some spectra.

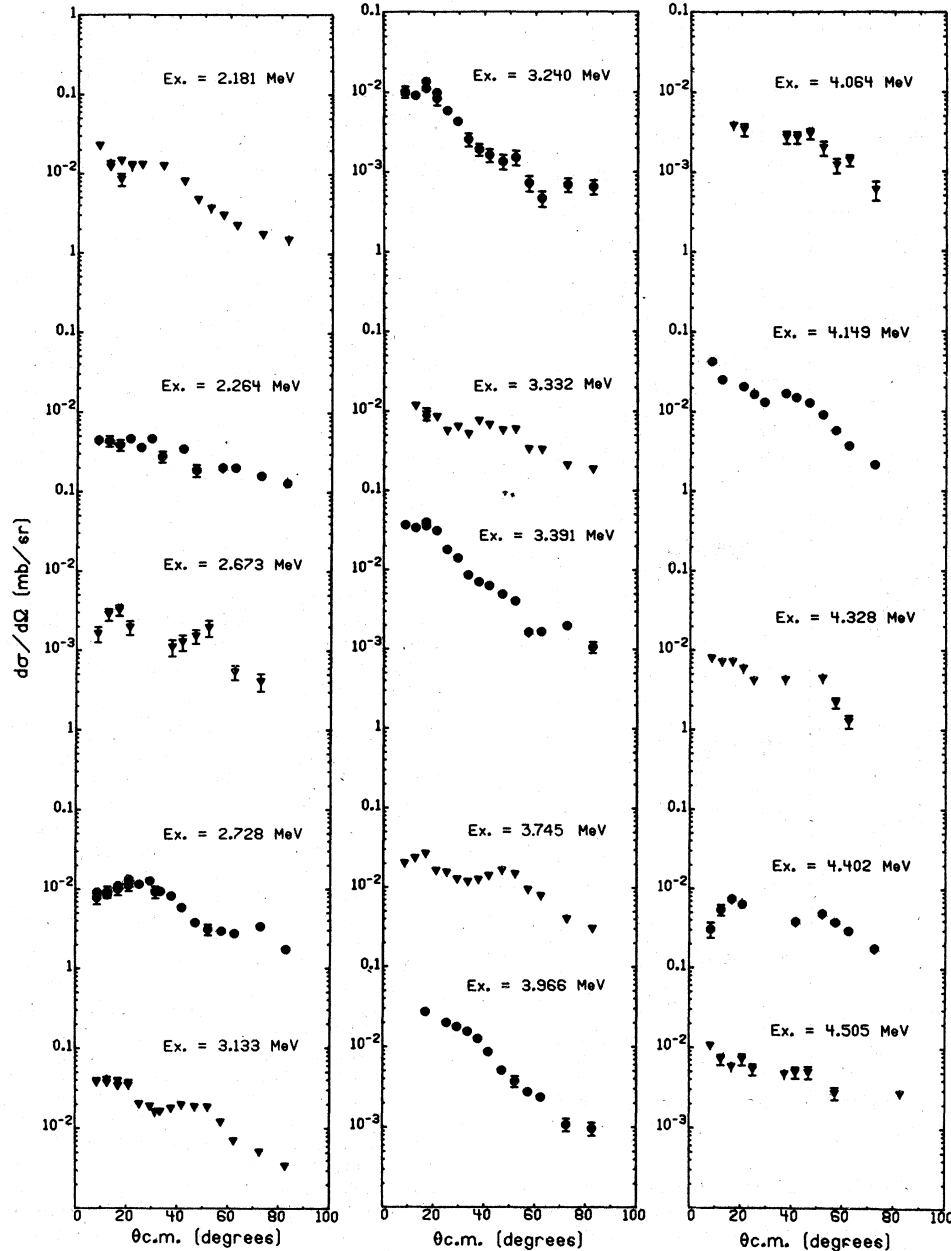


FIG. 4. Angular distributions for the $^{52}\text{Cr}(p,\alpha)^{49}\text{V}$ reaction to states with excitation energies between 2. and 4.505 MeV.

Both j -values that go with $\ell=7$ have been previously identified. The two known $15/2^-$ states are seen weakly while the $13/2^-$ level at 2.861 MeV is not seen in this experiment.

There have not been any previous spin assignments for states to be reached by $\ell=6, 8$, or 9 transfers.

Alternation of strength is clearly evident for negative parity states. For a given ℓ -transfer, the j_{\downarrow} member is the strongest.

C. DWBA with Cluster Form Factors

It has been shown that zero-range DWBA calculations can be used to obtain reasonable fits to (p,α) angular distributions (see, for example, References 9, 29, 34, 44). In addition, finite range effects have been found to produce only minor changes in the shapes of the DWBA calculations.^{36, 45} Mass-3 cluster form factors have been used frequently for these calculations because they are

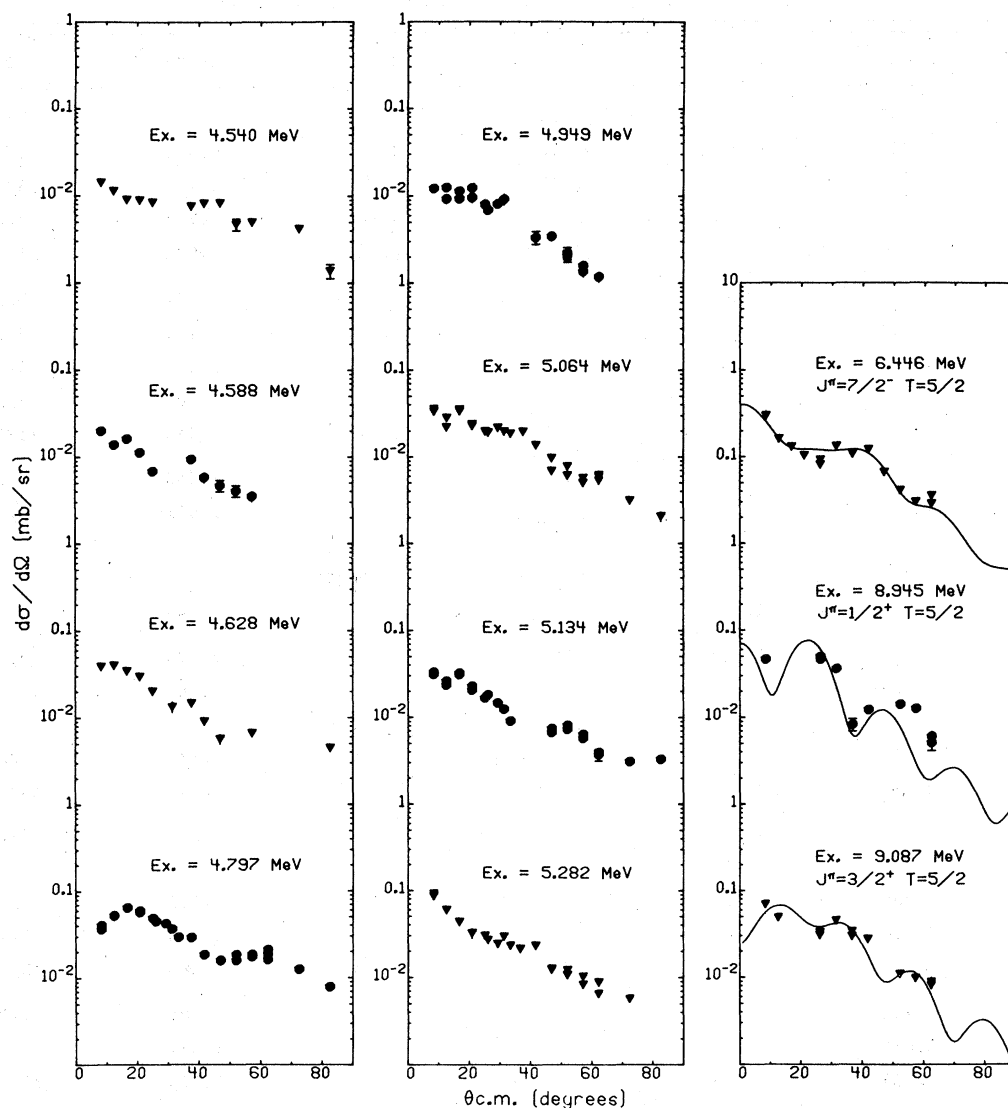


FIG. 5. Angular distributions for the $^{52}\text{Cr}(p,\alpha)^{49}\text{V}$ reaction to states with excitation energies of 4.540 MeV and above. The solid curves are DWBA calculations with cluster model form factors for the three isobaric analog states.

easy to generate. In addition, most researchers have found the radius and diffuseness parameters of the bound state well to be useful variables. These are usually varied to obtain the best overall fit to all the known levels. A wide variety of these parameters have been used (see References 34, 44). Many different sets of α -particle optical potentials have been tried which vary from shallow real wells of about 50 MeV depth to deep wells of 200 MeV depth. For the most part the choice of α -optical potential determines the values of the bound state well parameters that will best fit the data.

A simple, consistent method of generating reasonable calculations is needed. We have, therefore, set out to find a general procedure that can be used to get first order fits reliably.

Since angular momentum matching is a problem for the (p,α) reaction, it seems reasonable to try the "well matching" procedure for choosing the optical potentials and the bound state parameters. This procedure has been suggested by Dodd and Greider⁴⁶ and by Stock et al.⁴⁷ for reactions that are poorly matched. The method has been successfully applied to the (d,α) reaction.⁴⁸

The α -particle optical potential was taken to be a set with roughly 200 MeV real well depth. The well matching procedure requires that the radius and diffuseness of all the real potentials be the same. Alpha-scattering data of Fernandez and Blair⁴⁹ were refit to find an optical potential that met these well matching requirements. Since the α -elastic scattering could not be reproduced as well with a radius parameter of 1.17 fm as with 1.22 fm,

Table 1. Levels of ${}^{49}\text{V}$, excitation energies in MeV.

$(p,\alpha)^a$	$(p,t)^b$	$(t,\alpha)^c$	$({}^3\text{He},d)^c$	$(p,\gamma)^d$	$(\alpha,p\gamma)^e$	J^π
0.000	0.000	0.000	0.000			$7/2^-$
0.091	0.091	0.090	0.092	0.091	0.091	$5/2^-$
0.153	0.153	0.153	0.155	0.153	0.153	$3/2^-$
0.748		0.752	0.750	0.747	0.748	$3/2^+$
1.021	1.020	1.025	1.025	1.021	1.022	$11/2^-$
1.141		1.148		1.140	1.141	$5/2^+$
	1.154			1.155	1.155	$9/2^-$
1.513	1.516	1.531		1.514	1.515	$5/2^-$
1.602		1.610			1.603	$7/2^+$
				1.644	1.643	$(1/2^-)$
1.646		1.652			1.646	$1/2^+$
	1.662		1.672	1.661	1.661	$3/2^-$
				1.770(?)		
				1.796(?)		
1.995		1.999		1.996	1.995	$3/2^+$
2.181		2.189	2.193		2.179	$9/2^+$
	2.183				2.183	$7/2^-$
			2.204			
2.235	2.235	2.241		2.235	2.235	$5/2^-$
2.264	2.263	2.266			2.263	$15/2^-$
					2.265	$3/2^-$
			2.279			
2.308	2.306	2.314	2.317	2.309	2.310	$3/2^-$
2.354	2.350	2.358			2.353	$9/2^-$
2.386		2.394		2.388	2.388	$5/2^+$
2.406	2.404				2.408	$7/2^-$
2.673	2.666	2.681			2.671	
2.728	2.727	2.736			2.728	$(15/2^-)$
					2.741	
					2.786	
	2.811	2.812		2.808	2.811	
	2.861				2.861	
	3.020				3.017	
3.133	3.136	3.132	3.137		3.1334	$(11/2^-)$
					3.1337	$(11/2^-)$
3.240	3.241	3.248	3.248	3.237		$7/2^-$
					3.259	
	3.305					
3.330	3.332					
3.346	3.347	3.345			3.342	
3.391	3.398	3.388	3.401	3.390		
	3.479	3.465				
3.499						

Table 1. (Continued)

$(p, \alpha)^a$	$(p, t)^b$	$(t, \alpha)^c$	$({}^3\text{He}, d)^c$	$(p, \gamma)^d$	$(\alpha, p\gamma)^e$	J^π
3.525	3.534					
3.612	3.609					$(\geq 11/2^-)^a$
	3.624					
3.639	3.649					
3.673	3.685					
3.694		3.699				
	3.720					
3.745			3.748	3.744		$(\geq 9/2)^a$
	3.757	3.763		3.757		
	3.795					
	3.825			3.816		
3.838				3.840		
3.882	3.886					
	3.910			3.914		
3.934		3.929	3.922			
3.965	3.975	3.976				
4.004		4.005	4.012	4.006		
	4.048	4.042				
4.064						
	4.098	4.090				
			4.135	4.127		
4.149		4.153				
	4.165					
	4.209					
			4.224			
			4.253	4.250		
4.268 ^{g)}	4.277	4.280				
	4.305					
4.326						
4.375			4.375	4.373		
4.400		4.402				
4.436			4.448 ^{h)}			
4.470						
4.501		4.511	4.502	4.498		
4.538	4.538					
4.588		4.587	4.590			
			4.599			
4.628 ^{g)}			4.639			
		4.646	4.645			
4.662						
		4.860				
4.755		4.743				

Table 1. (Continued)

(p, α) ^{a)}	(p,t) ^{b)}	(t, α) ^{c)}	($^3\text{He},d$) ^{c)}	(p, γ) ^{d)}	($\alpha,p\gamma$) ^{e)}	J ^π
4.797					($>11/2$) ^{a)}	
4.830		4.838				
4.863		4.871	4.852			
4.885						
4.949		4.959	4.945			
4.988						
5.010	5.018	5.017				
	5.072					
5.134		5.146	5.130			
5.204			5.216			
		5.239				
5.282	5.285	5.289	5.257			
5.347						
		5.355				
		5.375	5.370			
5.387						
5.411			5.403			

6.446			6.474			$7/2^-, T=5/2^a)$
8.945						$1/2^+, T=5/2^a)$
9.087						$3/2^+, T=5/2^a)$

a) This Expt.

b) Ref. 11

c) Ref. 12

d) Ref. 19

e) Ref. 16

f) Errors are ± 0.003 MeV for states below 3 MeV, ± 0.006 MeV for states above 3 MeV, and ± 0.025 MeV for the $T=5/2$ states.

g) The peak is an unresolved doublet. It's width is too large to be a single peak.

h) Correspondence is unsure.

Table 2. Levels seen in $^{52}\text{Cr}(p,\alpha)^{49}\text{V}$ that are not in $^{51}\text{V}(p,t)^{49}\text{V}$ ^{a)}

Excitation Energy	J
0.748	$3/2^+$
1.141	$5/2^+$
1.602	$7/2^+$
1.646	$1/2^+$
1.995	$3/2^+$
2.388	$5/2^+$

a) Ref. 11

the second preferred proton set of Becchetti and Greenlees⁵⁰ was used. Using this prescription, the bound state wave function should be calculated in a well with $r_0=1.22$ fm. and a diffuseness of 0.72 fm to agree with the other potentials. The triton well depth should ideally be about 150 MeV, however, after adjustment to reproduce the triton separation energy, it was usually between 120 MeV and 140 MeV. The optical potentials are given in Table 4.

The shapes which were obtained using this procedure were generally satisfactory. However, the forward angle behaviour of the $7/2^-$ calculation did not increase as the angle decreased. Most of the searching on the bound state parameters that has been done by other researchers has resulted in smaller diffuseness than was used above. If the diffuseness is decreased to 0.65 fm, the $7/2^-$ calculation has the correct forward angle behaviour. In other words, the forward angles are sensitive to the diffuseness. The fits obtained with this choice are indicated by the solid curves in Figures 3 and 5. Calculations with smaller diffuseness were found to produce more pronounced

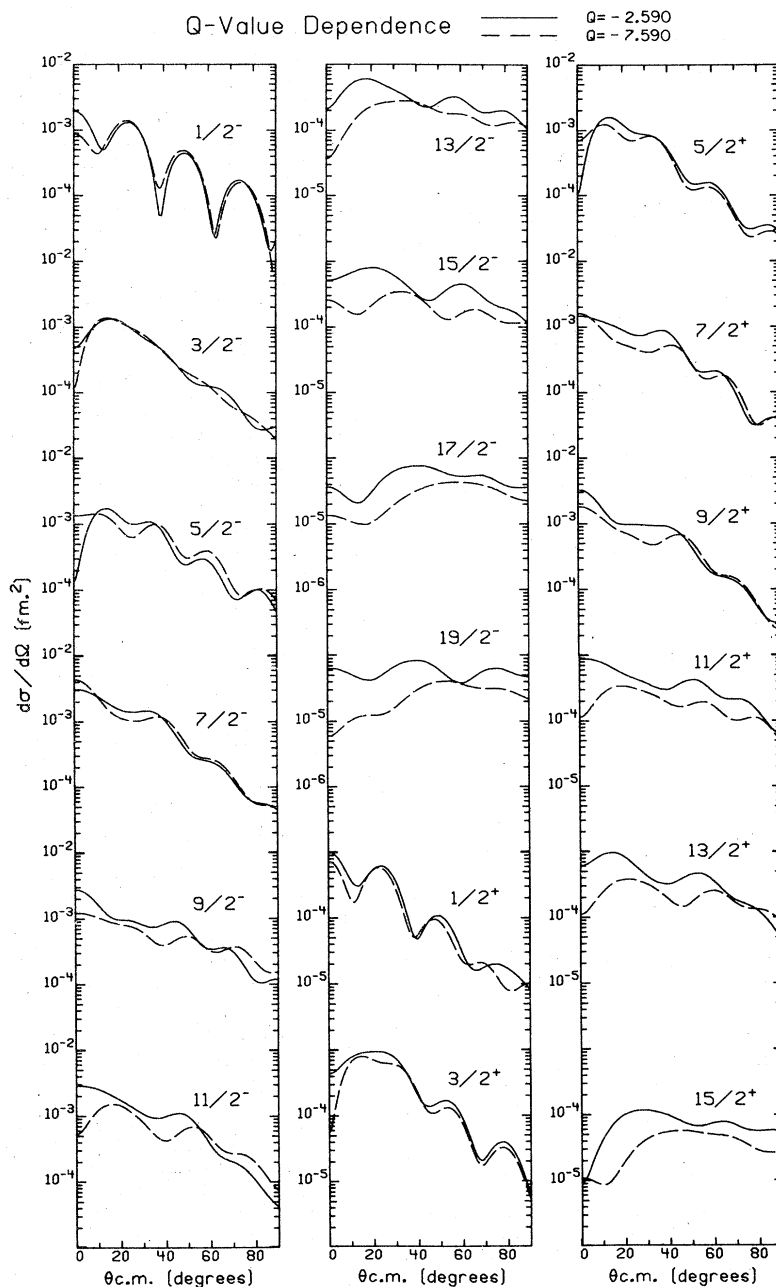


FIG. 6. Sample DWBA calculations with cluster model form factors to illustrate L- and J-dependence of the (p, α) reaction. The calculations are for a Q-value corresponding to the ground state transition (solid lines) and for one corresponding to 5 MeV excitation (dashed lines).

oscillations.

Sensitivity of this kind is a characteristic of reactions that suffer from a severe angular momentum mismatch. Semi-classical angular momentum matching occurs for the ground state Q-value at $L \approx 6$. Angular momentum mismatch may also imply a strong Q dependence of the cross sections, with higher excitation energies corresponding to less angular momentum mismatch and, therefore, larger cross sections. Even though cluster model calculations are not particularly useful when

comparing the strengths of individual transitions, their energy dependence should be meaningful. Figure 6 shows a comparison of DWBA calculations assuming no excitation to a set calculated with 5 MeV excitation. No strong dependence on excitation energy is observed, though there are some small changes in predicted shapes. Possibly the increased triton binding partially compensates for the better angular momentum matching. It is also true that the angular momentum matching criterion is less important in (p, α) reactions than it is in

Table 3. Levels seen in either $^{51}\text{V}(p, t)^{49}\text{V}$ ^{a)} or $^{50}\text{Cr}(t, \alpha)^{49}\text{V}$ ^{b)} but not observed in $^{52}\text{Cr}(p, \alpha)^{49}\text{V}$.

Excitation Energy	J
1.154 ^{c)}	9/1 ⁻
1.662 ^{c)}	3/2 ⁻
2.786	(9.2, 11/2) ⁻
2.811 ^{d)}	(5/2, 7/2) ⁻
2.861 ^{c)}	(13/2) ⁻
3.020 ^{c)}	(3/2, 7/2) ⁻
3.305 ^{c)}	
3.479 ^{c)}	7/2 ⁻
3.624 ^{c)}	
3.720 ^{c)}	
3.825 ^{c)}	
3.910 ^{c)}	
4.048 ^{d)}	
4.098 ^{d)}	
4.165 ^{c)}	
4.209 ^{c)}	
4.305 ^{c)}	

a) Ref. 11

b) Ref. 12

c) Not seen in (p, t) data

d) Not seen in either (p, t) or (t, α) data

reactions involving 2 strongly absorbed particles such as in ($^3\text{He}, \alpha$) reactions.³⁶ It is interesting to note that the change in shape for the 7/2⁻ forward angle behaviour is similar to what is actually observed for the 6.446 MeV state.

D. DWBA with Microscopic Form Factors

The cluster model is useful for studying the effects of optical potentials and the bound state well shape,

however, the relative strengths of states are difficult to predict with such a model. Significant progress along these lines has recently been made via the development of a semi-microscopic model which utilizes weak coupling wave functions and cluster form factors.^{9, 35} Microscopic models, however, are still necessary to predict the relative strengths of states from detailed shell model wavefunctions. Such models are also essential in evaluating possible dependence of angular distribution shapes on detailed configuration structure. Because microscopic form factors do not have the shape flexibility that the cluster form factors have, it is advisable to use "well matched" optical parameters, since they are the least sensitive to form factor shapes.

Microscopic models which use single particle wavefunctions generated in Woods-Saxon wells have been developed previously.^{25, 30, 36} In Reference 36 and the present work the two neutrons are coupled together to make a di-neutron using the two nucleon form factor method of Bayman and Kallio,³⁷ and the di-neutron is then treated as a mass two particle and coupled to the proton to make a triton in a 0s internal state by a modification of the two nucleon technique. This is, in principle, equivalent to the expansion of Woods-Saxon radial functions in terms of oscillator functions as in References 25 and 30.

DWBA calculations utilizing microscopic form factors are shown as dashed curves in Figure 3. The fits are comparable or somewhat worse than the cluster fits shown as solid curves.

The calculation of strengths requires detailed spectroscopic amplitudes from shell model wave functions. However, the hole state yields may be calculated as simple seniority one transfers, if we assume that the two neutrons picked up are coupled to zero angular momentum. This is equivalent to neglecting the more complicated components of the hole states in which the neutrons may be coupled to non-zero angular momentum. With this assumption, the relative strengths for the 7/2⁻, 3/2⁺, and 1/2⁺ proton hole states should be the same as would be expected for the $^{50}\text{Cr}(d, ^3\text{He})^{49}\text{V}$ or $^{50}\text{Cr}(t, \alpha)^{49}\text{V}$ reactions. The hole state relative spectroscopic factors are given in Table 5. The agreement with the expected values is very good, thus the simple seniority one assumption seems to be reasonable for these states. As discussed in Reference 9, the relative yields in (p, α) may be different than in simple proton pickup when the (p, t) reaction strongly populates 2⁺ states.

It is of interest to compare the relative yields predicted in the microscopic models for states of various J ^{π} with pure 0f_{7/2} transfers. We have, therefore, computed all the 0f_{7/2} form factors and performed DWBA calculations with these form factors. The peak cross sections predicted by these calculations are tabulated in Table 6.

Table 4. Optical Potentials^{a)}

	V	r _o	a	V _{so}	r _{so}	a _{so}	W	r _{si}	a _i	W _{sf}
proton	43.22	1.22	0.72	-25.0	1.01	0.75	-5.0	1.32	0.52	12.60
alpha	196.34	1.22	0.72				-15.72	1.76	0.42	
"triton"	V _t ^{b)}	1.22	0.72	0						

a) V and W include the factor of 4 necessary for using the code DWUCK.⁵³

b) Adjusted to fit triton separation energy.

Table 5. Relative Spectroscopic Factors

Excitation Energy	J	Zero-order	(p,α)	(t,α) ^{b)}
0.000	7/2 ⁻	4.	4.	4. a)
0.748	3/2 ⁺	4.	3.4	3.7
1.646	1/2 ⁺	2.	2.2	2.1

a) Normalized to 4. All other values relative to this.

b) Reference 12.

Notice that the 19/2⁻ is much larger than the 17/2⁻ prediction. The trend that the $j_>$ strengths are greater than the $j_<$ strengths seems to be general. This "j-dependence" in the magnitudes of the cross sections is experimentally observed, e.g. in the 11/2⁻, 9/2⁻ case, as was mentioned previously in the j-dependence discussion. This predicted alternation is due to the internal vector coupling of the proton and neutron angular momenta to the total J value.

These calculations indicate the likelihood of observing a 19/2⁻ level. Comparing the DWBA calculations for the 19/2⁻ transfer and the seniority one 7/2⁻ transfers shows that the ground state is predicted to be 48 times stronger than the 19/2⁻ at 12° while the 19/2⁻ is expected to be 6 times larger than the 7/2⁻ at 70°. The fact that we have not unambiguously located such a strong 19/2⁻ level is possibly due to dilution of this predicted (p,α) strength into several more complicated 19/2⁻ states. Several such states are predicted in ⁴⁹V by References 41 and 42. A simpler 19/2⁻ state is expected in ⁴³Sc and in fact a relatively strong transition is seen in the ⁴⁰Ca(α,p) reaction.³⁹ Seniority one transitions, e.g. 7/2⁻, 3/2⁺, and 1/2⁺ states can also be enhanced over high spin states by the coherence of L=0 coupled neutron configurations which causes the strong L=0 transitions in (p,t) reactions.

Table 6. Peak (p,α) Cross Sections for (0f_{7/2})³ Configurations. a)

J	ℓ ₁₂ =				
	0	2	4	6	
1/2 ⁻			1.132		
3/2 ⁻		.796	.214		
5/2 ⁻		.076	.152	.291	
7/2 ⁻	1.0	.283	.122	.044	
9/2 ⁻		.047	.087	.114	
11/2 ⁻		.401	.137	.055	
13/2 ⁻			.030	.041	
15/2 ⁻			.346	.102	
17/2 ⁻				.029	
19/2 ⁻				.279	

a) All values are relative to the J^π=7/2⁻; ℓ₁₂=0 maximum cross section. The values are σ_{DWUCK}/(2J+1).

E. The Population of Analog States

The isobaric analogs of states in ⁴⁹Ti are populated selectively in the high excitation region of the present spectra, as shown in Figure 2. The excitation energies of these three states are given in Table 1. A precision measurement of the ground state analog excitation energy⁵⁵ in ⁴⁹V is within 15 keV of the presently determined value. The fact that most of the previously known analog states²⁰⁻²⁴ in ⁴⁹V were not populated appreciably in this work is consistent with the tendency of the (p,α) reaction to populate simpler hole-state configurations. That the three states seen here are indeed analog states is supported by the energy comparisons given in Table 7.

A significant feature of the analog states observed here is their large cross sections. The yields of the 7/2⁻, 3/2⁺, and 1/2⁺ analog states shown in Figure 5 are actually in each case equal to or larger than those for the corresponding T_< states in Figure 3. In the single neutron transfer work of Sherr et al.,⁵² for example, the cross section of the 7/2⁻ (T_>) level in ⁵²Cr(p,d) was about 1/20 that of the ground state, which was the strongest 7/2⁻ (T_<) state. (Of this factor of 20, about a factor of 3 was explained by DWBA kinematics and about a factor of 6 by the shell model spectroscopic amplitudes.) Sum rules for the yields to T_> and T_< levels in single nucleon transfer⁵³ predict a yield of π(2T+1)⁻¹ ≈ 0.8 to the 7/2⁻ (T_>) state in ⁵¹Cr, and a yield of ν-π(2T+1)⁻¹ ≈ 7.2 for the sum of the 7/2⁻ (T_<) state, where π and ν represent the number of f_{7/2} protons and neutrons, respectively, in ⁵²Cr.

For the (p,α) reaction such sum rules do not exist because of the coherence in the internal degrees of freedom, but by using simple seniority estimates of the spectroscopic factors^{2,43} yields of the strongest states can be estimated. In this approximation the yield to the 7/2⁻ state in ⁴⁹Ti reached via a ³He pickup reaction on ⁵²Cr would be ≈ 8 (1.25), where the first factor is the neutron spectroscopic factor for the full f_{7/2} neutron shell and the second is the two proton spectroscopic

Table 7. Analog States in ⁴⁹V seen via the (p,α) reaction. a)

	⁴⁹ V		⁴⁹ Ti	Coulomb Energy
	E _x ^{b)}	E _x -6.431	E _x ^{c)}	E _c ^{b)}
7/2 ⁻	6.431(5)	0.	0.	7.815(4)
1/2 ⁺	8.932(20)	2.501	2.503(8)	7.813(22)
3/2 ⁺	9.073(20)	2.642	2.665(8)	7.782(22)

a) Energies are given in MeV. Other analog states in ⁴⁹V have been reported in References 19 through 24.

b) The ground state coulomb energy given here is from Reference 54 measured via (³He,t). The number given here has been corrected for the change in the reference reaction Q-value ⁴²Ca(³He,t), reported in Reference 55. The excitation energies from the present work have been shifted downwards by 15 keV to correspond with this more accurate scale.

c) See Reference 56 and references therein.

factor for the half full $f_{7/2}$ proton shell. The analog of this state in ^{49}V is the $7/2^- (T_>)$ state seen here via the triton pickup reaction. It would have the yield of its parent state reduced by the isospin coupling factor, i.e., $8(1.25)/(2T+1) \approx 2$. In this approximation the total yield to the $T_>$ and $T_<$ $j^\pi = 7/2^-$ states via triton pickup is $\approx 4(1.0)$ where the first factor is the proton spectroscopic factor for the half full $f_{7/2}$ proton shell and the second is the two neutron factor for the full $f_{7/2}$ neutron shell. This total yield estimate combines with the above $T_>$ yield estimate to leave a prediction of ≈ 2 for the $7/2^- (T_<)$ state. Thus the simple model predicts approximately equal population of the $T_<$ and $T_>$ $7/2^-$ levels in the (p, α) reaction. The ratio extracted via DWBA with cluster model form factors is ≈ 2.4 for the separation energy prescription and ≈ 0.7 with the effective binding prescription.⁵² This agreement is good, especially for the latter calculation, considering the very simple wave functions assumed above.

IV. CONCLUSIONS

The proton hole states have been found to dominate the $^{52}\text{Cr}(p, \alpha)^{49}\text{V}$ spectra at forward angles. This observation agrees with those of others that have studied the (p, α) reaction in the $1p$ -shell. Many weak transitions are observed with differential cross sections of $\approx 10 \mu\text{b}/\text{sr}$.

The (p, α) reaction has been shown to have a high degree of selectivity. A number of levels that are observed with significant strength in $^{51}\text{V}(p, t)^{49}\text{V}$ were not observed in the (p, α) spectra. Turning this comparison around has proven to be a useful tool for finding positive parity states, none of which appear in the (p, t) spectra.

Peaks which are relatively more prominent in the back angle spectra have been observed, and are candidates for high spin states, such as $19/2^-$, $15/2^-$, or $15/2^+$.

Little evidence for j -dependence for $\ell=2$ and $\ell=3$ transfers has been found. If j -dependence exists, it is subtle and at a level such that structure effects can be equally important.

DWBA calculations using cluster form factors have been shown to reproduce the shapes of the angular distributions of the known levels reasonably well.

The relative population of analog states in this reaction was about 10 times stronger than in the (p, d) reaction on the same target. This difference was qualitatively explained via comparison of expected yields in ^3He as triton pickup reactions with the assumptions of simple seniority wave functions and spectroscopic factors.

Microscopic form factors have been tested with zero-order shell model assumptions. DWBA calculations using these form factors have been shown to reproduce the shapes of the angular distributions with quality slightly inferior to the cluster model fits. Relative spectroscopic factors for the $T=3/2$ proton hole states have been derived from the microscopic calculations and are found to be in agreement with single proton pickup.

Finally a qualitative feature of j -dependent strength is observed. The $j_>$ member of the $\ell=1, 3, 5$ transfers is generally stronger than the $j_<$ member. The microscopic model based on $0f_{7/2}$ pure configurations predicts this qualitative effect, which explains, for example, the observance of many relatively strong $11/2^-$ transitions but very few $9/2^-$ states in (p, α) and (α, p) studies in the $0f_{7/2}$ shell.

ACKNOWLEDGMENTS

This material is based upon work supported by the National Science Foundation under Grant No. Phy 78-01684.

*Present address, Nuclear Physics Laboratory, University of Colorado, Boulder, CO.

†Present address, McMaster University, Hamilton, Ontario.

¹L.L. Lee Jr., A. Marinov, C. Mayer-Boricke, J.P. Schiffer, R.H. Bassel, R.M. Drisko, and G.R. Satchler, Phys. Rev. Lett. **14** 261(1965).

²J.A. Nolen, Jr. Thesis, Princeton University (1965) unpublished.

³J.A. Nolen, Jr., C.M. Glashauser and M.E. Rickey, Phys. Lett. **21**(1966) 705.

⁴L.S. August, P. Shapiro, and L.R. Cooper, Phys. Rev. Lett. **23** 537(1969).

⁵G. Brown, A. MacGregor, and R. Middleton, Nucl. Phys. **A77** 385(1966).

⁶G. Brown, S.E. Warren, and R. Middleton, Nucl. Phys. **A77** 365(1966).

⁷R.W. Tarara, J.D. Goss, P.L. Jolivet, G.F. Neal, and C.P. Browne, Phys. Rev. C **13** 109(1976).

⁸J.D. Goss, P.L. Jolivet, A.A. Rollefson, and C.P. Browne, Phys. Rev. C **10** 2641(1974).

⁹J.W. Smits and R.H. Siemssen, Nucl. Physics **A261** 385(1976), and J.W. Smits, Thesis, University of Groningen 1977 unpublished.

¹⁰R.G. Markham, R.K. Bhowmik, M.A.M. Shahabuddin, P.A. Smith, and J.A. Nolen, Jr., Bull. Am. Phys. Soc. **21** 634(1976).

¹¹A. Saha, H. Nann, and K.K. Seth, private communication.

¹²D. Bachner, R. Santo, H.H. Duhm, R. Bock, and S. Hinds, Nucl. Phys. **A106** 577(1968).

¹³N.H. Prochnow, H.W. Newson, E.G. Bilpuch, and G.E. Mitchell, Nucl. Phys. **A194** 353(1972).

¹⁴Z.P. Sawa, J. Blomqvist, and W. Gullholmer, Nucl. Phys. **A205** 257(1972).

¹⁵J.G. Malan, E. Barnard, J.A.M. deVilliers, J.W. Tepel, and P. Van der Merwe, Nucl. Phys. **A195** 596(1972).

¹⁶B. Haas, J. Chevallier, J. Britz, and J. Styczen, Phys. Rev. C **11** 1179(1975).

¹⁷S.R. Tabor and R.W. Zurmuhle, Phys. Rev. C **10** 35(1974).

¹⁸B. Haas, J. Chevallier, N. Schulz, J. Styczen, and M. Toulemonde, Phys. Rev. C **11** 280(1975).

¹⁹C. Rossi-Alvarez and C.B. Virgiani, Il Nuovo Cimento **17A** 721(1973).

²⁰H.V. Klapdor, Nucl. Phys. **A114** 673(1968), and Nucl. Phys. **A134** 419(1969).

²¹L. El Nadi and M.A. Harith, private communication.

²²S. Gales, S. Fortier, H. Laurent, J.M. Maison, and J.P. Schapira, Nucl. Phys. **A259** (1976) 189.

²³D.J. Pullen, B. Rosner, and Ole Hansen, Phys. Rev. **166** 1142(1968).

²⁴S. Maripu, Nucl. Phys. **A153** 183(1970).

²⁵W.R. Falk, Phys. Rev. C **8** 1757(1973).

²⁶B. Bardin, Thesis, University of Colorado 1964 unpublished.

²⁷B.F. Bayman, Nuclear Spectroscopy with Direct Reactions II, Argonne National Lab. Report ANL-6878 335(1964).

²⁸J.J. Kolata, J.W. Olness, and E.K. Warburton, Phys. Rev. C **10** 1663(1974).

- ²⁹R.J. Peterson and H. Rudolph, Nucl. Phys. A241 253 (1975).
- ³⁰W.R. Falk, A. Djalois, and D. Ingham, Nucl. Phys. A252 452 (1975).
- ³¹K. van der Borg, R.J. de Meijer, and A. van der Woude, Nucl. Phys. A273 172 (1976).
- ³²L.S. August, P. Shapiro, L.R. Cooper, and C.D. Bond, Phys. Rev. C 4 2291 (1971).
- ³³R.K. Bhowmik, J.A. Nolen, Jr., P.A. Smith, R.G. Markham, and M.A.M. Shahabuddin, Bull. Am. Phys. Soc. 20 1164 (1975).
- ³⁴Michel Vergnes, Georges Rotbard, Jacques Kalifa, and Genevieve Barrier-Rossin, Phys. Rev. C 10 1156 (1974).
- ³⁵J.W. Smits, F. Iachello, R.H. Siemssen, and A. van der Woude, Phys. Lett. 53B 337 (1974).
- ³⁶P.A. Smith, Thesis, Michigan State University 1976 unpublished.
- ³⁷B.F. Bayman and A. Kallio, Phys. Rev. 156 1121 (1967).
- ³⁸R.G. Markham and R.G.H. Robertson, Nucl. Instr. and Meth. 129 (1975) 131.
- ³⁹P.A. Smith and R.J. Peterson, Bull. Am. Phys. Soc. 22 633 (1977) and I. Fischman, C.E. Thorn, A.M. Bernstein, and D. Cline, Phys. Lett. 41B 298 (1972).
- ⁴⁰G. Fortuna, S. Lunardi, M. Morando, and C. Signorini unpublished.
- ⁴¹J.D. McCullen, B.F. Bayman, and Larry Zamick, Princeton University Technical Report NYO-9891 (1964), and Phys. Rev. 134 B515 (1964).
- ⁴²W. Kutschera, B.A. Brown, K. Ogawa, submitted to Rivista del Cimento, private communication.
- ⁴³R. Sherr, Proceedings of the Conference on Direct Interactions and Nuclear Reaction Mechanisms, University of Padua, edited by E. Clemental and C. Villi (1962) 1025.
- ⁴⁴Yong Sook Park, H.D. Jones, and D.W. Bainum, Phys. Rev. C 7 445 (1973).
- ⁴⁵R.M. Drisko and G.R. Satchler, Phys. Lett. 9 342 (1964).
- ⁴⁶K.R. Greider, L.R. Dodd, Phys. Rev. 146 671 (1966) and L.R. Dodd and K.R. Greider, Phys. Rev. 146 675 (1966).
- ⁴⁷R. Stock, R. Boch, P. David, H.H. Duhm, and T. Tamura, Nucl. Phys. A104, 136 (1967).
- ⁴⁸R.M. Del Vecchio and W.W. Daehnick, Phys. Rev. C 6 1095 (1972).
- ⁴⁹B. Fernandez and J.S. Blair, Phys. Rev. C 1 523 (1970).
- ⁵⁰F.D. Becchetti and G.W. Greenlees, Phys. Rev. 182 1190 (1969).
- ⁵¹P.D. Kunz, unpublished.
- ⁵²R. Sherr, B.F. Bayman, E. Rost, M.E. Rickey, and C.G. Hoot, Phys. Rev. 139 B1272 (1965).
- ⁵³J.P. Schiffer, Isospin in Nuclear Physics edited by D.H. Wilkinson
- ⁵⁴F.D. Becchetti, D. Dehnhard, and T.G. Dzubay, Nucl. Phys. A168 151 (1971).
- ⁵⁵H. Vonach, P. Glassel, E. Huenges, P. Maier-Komor, H. Rosler, H.J. Scheerer, H. Paul, and D. Semrad, Nucl. Phys. A278 189 (1977).
- ⁵⁶P.J. Plauger and E. Kashy, Nucl. Phys. A152 609 (1970).